Sparse NOMA: A Closed-Form Characterization

Shlomo Shamai (Shitz)
The Andrew and Erna Viterbi Faculty of Electrical Engineering
Technion—Israel Institute of Technology

Joint work with

Benjamin M. Zaidel, The Alexander Kofkin Faculty of Engineering, Bar Ilan University, Israel
and
Ori Shental, Communications Theory Department, Bell Labs, Holmdel, NJ,

Princeton, Department of Electrical Engineering Seminar

February 20, 2019

Introduction

Introduction

- Future wireless networks will be characterized by:
  - Dramatically higher throughputs
  - Emerging overloaded scenarios involving massive machine-type communications
- This immediately implies that the prevailing paradigms of orthogonal transmissions cease to apply:
  - More users than physical resources
- Non-orthogonal multiple-access (NOMA) is hence the key to future needs, see, e.g.:
  - [Saito, Kishiyama, Benjebbour, Nakamura, Li & Higuchi (2013)]
  - [Ding, Lei, Karagiannidis, Schober, Yuan & Bhargava (2017)]
  - [Wei, Yuan, Ng, Elkashlan & Ding (2016)]

NOMA Techniques

- NOMA techniques can be roughly categorized into two main classes:
  - Power-domain multiplexing (typically for the downlink):
    - Superposition coding combined with successive interference cancellation (SIC) at the receivers
    - Power allocation according to the respective channel conditions
  - Code-domain multiplexing:
    - Relies on distinguishing spreading codes (similar to CDMA or MC-CDMA), or interleaver sequences
    - Signals are multiplexed over the same time-frequency resources (e.g., in an OFDM framework)
- This work focuses on code-domain multiplexing

LDCD NOMA (Sparse NOMA)

- Low-density code-domain (LDCD) NOMA relies on low-density (sparse) signatures comprising a small number of non-zero elements
- Significant receiver complexity reduction can be achieved by utilizing message-passing algorithms (MPAs) [Bayesteh *et al.* (2015)]
- The scheme can be generally applied to any set of orthogonal resources, e.g., in the time, frequency, or space domain
- The sparse mapping between users and resources in LDCD-NOMA is dubbed:
    - Regular mapping:
        - Each user occupies a fixed number of resources
        - Each resource is used by a fixed number of users

LDCD NOMA (Sparse NOMA)

- Low-density code-domain (LDCD) NOMA relies on low-density (sparse) signatures comprising a small number of non-zero elements
- Significant receiver complexity reduction can be achieved by utilizing message-passing algorithms (MPAs) [Bayesteh *et al.* (2015)]
- The scheme can be generally applied to any set of orthogonal resources, e.g., in the time, frequency, or space domain
- The sparse mapping between users and resources in LDCD-NOMA is dubbed:
    - Irregular mapping:
        - The respective numbers are random, and only fixed on average

LDCD NOMA (Sparse NOMA)

- Low-density code-domain (LDCD) NOMA relies on low-density (sparse) signatures comprising a small number of non-zero elements
- Significant receiver complexity reduction can be achieved by utilizing message-passing algorithms (MPAs) [Bayesteh *et al.* (2015)]
- The scheme can be generally applied to any set of orthogonal resources, e.g., in the time, frequency, or space domain
- The sparse mapping between users and resources in LDCD-NOMA is dubbed:
  - Partly-regular mapping:
    - Each user occupies a fixed number of resources
    - Each resource is used by a random, yet fixed on average, number of users
    - The fixed and random aspects of the mapping can be switched

Motivation

- The optimal spectral efficiency of irregular LDCD-NOMA was investigated in [Yoshida & Tanaka (2006)] using the replica method of statistical physics
- It was shown to reside below the spectral efficiency of randomly spread code-division multiple-access (RS-CDMA) [Verdú & Shamai (1999)]
- The latter can be considered as a representative of dense NOMA
- Similar observations were also made for partly-regular time-hopping (TH) CDMA [Ferrante & Di Benedetto (2015)]

Motivation *Cont'd*

- The result stems from the random nature of the user-resource mapping:
  - Some users may end up without any designated resources
  - Some resources may be left unused
- Our objective was to investigate analytically the potential capacity gains of regular user-resource mappings
- For the sake of analytical tractability, we focus on the large system limit
- We extend here initial observations in [Shental, Zaidel & Shamai (2017)], mostly based on the heuristic "cavity method"[1] and numerical integration

[1] Applied in a statistical physics framework

The System Model

System Model

- Consider a system where the signals of K users ("layers") are multiplexed over N shared orthogonal resources (dimensions)
- The N-dimensional received signal at some arbitrary time instance is given by

$$\mathbf{y} = \sqrt{\frac{\mathsf{snr}}{d}}\,\mathbf{A}\mathbf{x} + \mathbf{n} \tag{1}$$

where:

- $\mathbf{x}$ is a K-dimensional vector comprising the coded symbols of the users:
  - We assume full symmetry, equal powers and no user cooperation
  - Independent Gaussian codebooks: $\mathbf{x} \sim \mathcal{CN}(\mathbf{0}, \mathbf{I}_K)$
- $\mathbf{n} \sim \mathcal{CN}(\mathbf{0}, \mathbf{I}_N)$ is the N-dimensional AWGN vector
- snr thus designates the per-user SNR at the receiver

System Model

- Consider a system where the signals of K users ("layers") are multiplexed over N shared orthogonal resources (dimensions)
- The N-dimensional received signal at some arbitrary time instance is given by

$$\mathbf{y} = \sqrt{\frac{\mathsf{snr}}{d}}\,\mathbf{A}\mathbf{x} + \mathbf{n} \tag{1}$$

where:

  - $\mathbf{A}$ is the $N \times K$ random sparse signature matrix:
    - The kth column represents the spreading signature of user k
    - User k occupies resource n if $A_{nk} \neq 0$
    - The system load is denoted by $\beta \triangleq K/N$

System Model

- Consider a system where the signals of K users ("layers") are multiplexed over N shared orthogonal resources (dimensions)
- The N-dimensional received signal at some arbitrary time instance is given by

$$\mathbf{y} = \sqrt{\frac{\mathsf{snr}}{d}}\,\mathbf{A}\mathbf{x} + \mathbf{n} \tag{1}$$

where:

  - The regularity assumption on $\mathbf{A}$ dictates that:
    - Each column has exactly $d \in \mathbb{N}^+$ non-zero entries ($d \geq 2$)
    - Each row has exactly $\beta d \in \mathbb{N}^+$ non-zero entries ($\beta d \geq 2$)
  - Note that in the corresponding irregular setting ($\mathbb{P}\{A_{nk} \neq 0\} = \frac{d}{N}$) the respective numbers are asymptotically Poissonian with averages d and βd

System Model

- Consider a system where the signals of K users (“layers”) are multiplexed over N shared orthogonal resources (dimensions)
- The N-dimensional received signal at some arbitrary time instance is given by

$$\mathbf{y} = \sqrt{\frac{\mathsf{snr}}{d}}\,\mathbf{A}\mathbf{x} + \mathbf{n} \qquad (1)$$

where:

- The nonzero entries $\mathbf{A}$ are assumed to be i.i.d. but otherwise arbitrarily distributed on the unit-circle in $\mathbb{C}$:
  - Repetition-based spreading and binary random spreading are special cases
  - The model may also account for phase-fading scenarios
- The columns of $\frac{1}{\sqrt{d}}\mathbf{A}$ are thus of unit norm
- $\mathbf{A}$ is assumed to be known at the receiving end

Construction of the Signature Matrix $\mathbf{A}$

- A key observation is that $\mathbf{A}$ can be associated with the adjacency matrix of a random $(\beta d, d)$-semiregular bipartite (factor) graph $\mathcal{A}$
- In this graph, a user node k and a resource node n are connected if and only if $A_{nk} \neq 0$
- The graph is assumed to be locally tree-like, and converge in the large system limit ($N \to \infty$) to a weighted bipartite Galton-Watson tree (BGWT) with:
  - Degree distribution $(\delta_{\beta d}, \delta_d)$
  - Parameter $\frac{1}{1+\beta}$
- This essentially implies that for large dimensions short cycles are rare (similar to LDPC codes [Richardson & Urbanke (2008)])

Construction of the Signature Matrix $\mathbf{A}$ *Cont'd*

- Reduced complexity iterative near-optimal multiuser detection is thus feasible, while applying MPAs over the underlying graph [Bayesteh *et al.* (2015)]
- This comes in sheer contrast to RS-CDMA [Verdú & Shamai (1999)], where the optimum receiver is prohibitively complex
- The matrix $\mathbf{A}$ is assumed to be uniformly chosen randomly and independently per each channel use from the respective set of $(\beta d, d)$-semiregular matrices

Asymptotic Spectral Density

The Stieltjes Transform

- The Stieltjes transform of a probability measure μ on $\mathbb{R}$ is defined as

$$m(z) = \int_{\mathbb{R}} \frac{1}{x - z} \, \mathrm{d}\mu(x) \ , \quad z \in \mathbb{C}^+ \tag{2}$$

- The measure μ can be recovered from $m(z)$ via the Stieltjes inversion formula

$$\mathrm{d}\mu(\lambda) = \frac{1}{\pi} \lim_{\epsilon \to 0^+} \ \mathrm{Im}(m(z))|_{z=\lambda+\mathrm{j}\epsilon} \, \mathrm{d}\lambda \tag{3}$$

- The limit here is in the sense of weak convergence of measures, namely, for continuity points $a < b$ of μ we have (see, e.g., [Tulino & Verdú (2004)])

$$\mu[a, b] = \lim_{\epsilon \to 0^+} \frac{1}{\pi} \int_a^b \mathrm{Im}(m(z))|_{z=\lambda+\mathrm{j}\epsilon} \, \mathrm{d}\lambda \tag{4}$$

A Useful Result on Locally Tree-Like Graphs

- Consider a sequence of random bipartite graphs $\{\mathcal{G}_N\}$, converging in law to a BGWT with:
  - Degree distribution $(\delta_{\beta d}, \delta_d)$
  - Parameter $\frac{1}{1+\beta}$
- Let $\mathbf{W}$ be an $N \times K$ complex random weight matrix independent of $\mathcal{G}_N$, with i.i.d. entries having finite absolute second moments
- Let the $(N+K) \times (N+K)$ weighted adjacency matrix of $\mathcal{G}_N$ read

$$\tilde{\mathbf{A}}_N = \begin{pmatrix} \mathbf{0} & \mathbf{A} \\ \mathbf{A}^\dagger & \mathbf{0} \end{pmatrix} \triangleq \begin{pmatrix} \mathbf{0} & \mathbf{W} \\ \mathbf{W}^\dagger & \mathbf{0} \end{pmatrix} \circ \begin{pmatrix} \mathbf{0} & \bar{\mathbf{A}} \\ \bar{\mathbf{A}}^\dagger & \mathbf{0} \end{pmatrix} \tag{5}$$

where $\circ$ denotes the Hadamard product, and $\bar{\mathbf{A}}$ is a corresponding $(0,1)$-matrix

A Useful Result on Locally Tree-Like Graphs

Cont'd

- Let $\mathcal{H}$ denote the set of holomorphic functions $f : \mathbb{C}^+ \to \mathbb{C}^+$ such that $|f(z)| \leq \frac{1}{\mathrm{Im}(z)}$
- Let $\mathcal{P}(\mathcal{H})$ denote the space of probability measures on $\mathcal{H}$

Theorem 1 (Bordenave & Lelarge (2010), Theorems 4 & 5)

1. *There exists a unique pair of probability measures* $(\mu_a, \mu_b) \in \mathcal{P}(\mathcal{H}) \times \mathcal{P}(\mathcal{H})$ *such that for all* $z \in \mathbb{C}^+$

$$Y^a(z) \overset{d}{=} -(z + \sum_{i=1}^{\beta d-1} \left|W_i^b\right|^2 Y_i^b(z))^{-1} \tag{6}$$

$$Y^b(z) \overset{d}{=} -(z + \sum_{i=1}^{d-1} \left|W_i^a\right|^2 Y_i^a(z))^{-1} \tag{7}$$

where Y^a, Y_i^a *(respectively,* Y^b, Y_i^b*) are i.i.d. copies with law* μ_a *(respectively,* μ_b*), and* W_i^a, W_i^b *are i.i.d. random variables distributed as* W_{11}

A Useful Result on Locally Tree-Like Graphs

Cont'd

- Let $\mathcal{H}$ denote the set of holomorphic functions $f : \mathbb{C}^+ \to \mathbb{C}^+$ such that $|f(z)| \leq \frac{1}{\mathrm{Im}(z)}$
- Let $\mathcal{P}(\mathcal{H})$ denote the space of probability measures on $\mathcal{H}$

Theorem 1 (Bordenave & Lelarge (2010), Theorems 4 & 5)

2. *For all $z \in \mathbb{C}^+$, the Stieltjes transform $m_{\tilde{\mathbf{A}}_N}(z)$ of the empirical eigenvalue distribution of $\tilde{\mathbf{A}}_N$ converges as $N \to \infty$ in L^1 to $m_{\tilde{\mathbf{A}}}(z) = \frac{1}{1+\beta}\mathbb{E}\{X^a(z)\} + \frac{\beta}{1+\beta}\mathbb{E}\{X^b(z)\}$, where for all $z \in \mathbb{C}^+$*

$$X^a(z) \stackrel{d}{=} -(z + \textstyle\sum_{i=1}^{\beta d} \left|W_i^b\right|^2 Y_i^b(z))^{-1} \quad (5)$$

$$X^b(z) \stackrel{d}{=} -(z + \textstyle\sum_{i=1}^{d} |W_i^a|^2 Y_i^a(z))^{-1} \quad (6)$$

where Y_i^a, Y_i^b, W_i^a, and W_i^b are i.i.d. copies with laws as in Part (1)

Spectral Density of $\frac{1}{d}\mathbf{A}\mathbf{A}^\dagger$

- The bipartite graph $\mathcal{A}$ associated with the regular sparse spreading matrix $\mathbf{A}$ falls exactly within the framework considered in Theorem 1
- Furthermore, by the underlying assumption on the signatures, each i.i.d. entry of the corresponding weight matrix $\mathbf{W}$ has (surely) a unit absolute value
- This in turn implies that the recursive distributional equations (RDEs) in Theorem 1 admit a unique deterministic solution
- This deterministic solution yields a closed form expression for the limiting Stieltjes transform of the empirical eigenvalue distribution of $\tilde{\mathbf{A}}_N$

Spectral Density of $\frac{1}{d}\mathbf{A}\mathbf{A}^\dagger$ *Cont'd*

Theorem 2

- *Let the underlying assumptions of the regular sparse NOMA model hold*
- *Let* $2 \leq d \in \mathbb{N}^+ < \infty$, $2 \leq \beta d \in \mathbb{N}^+ < \infty$, $\alpha \triangleq \frac{d-1}{d}$ *and* $\gamma \triangleq \frac{\beta d - 1}{d}$
- *Assume that the weak limit of the associated bipartite graph* $\mathcal{A}$ *is a BGWT having degree distribution* $(\delta_{\beta d}, \delta_d)$ *and parameter* $\frac{1}{1+\beta}$. *Then:*

  1. *For all* $z \in \mathbb{C}^+$, *the Stieltjes transform of the empirical eigenvalue distribution of* $\frac{1}{d}\mathbf{A}\mathbf{A}^\dagger$ *converges as* $N \to \infty$ *in* L^1 *to*

$$m_{\frac{1}{d}\mathbf{A}\mathbf{A}^\dagger}(z) = -\left(z - \frac{\beta}{1+\alpha \mathsf{m}(z)}\right)^{-1}, \tag{7}$$

     where $\mathsf{m}(z)$ *solves the following deterministic equation:*

$$\mathsf{m}(z) = -\left(z - \frac{\gamma}{1+\alpha \mathsf{m}(z)}\right)^{-1} \tag{8}$$

Spectral Density of $\frac{1}{d}\mathbf{A}\mathbf{A}^\dagger$ *Cont'd*

Theorem 2

- *Let the underlying assumptions of the regular sparse NOMA model hold*
- *Let* $2 \leq d \in \mathbb{N}^+ < \infty$, $2 \leq \beta d \in \mathbb{N}^+ < \infty$, $\alpha \triangleq \frac{d-1}{d}$ *and* $\gamma \triangleq \frac{\beta d-1}{d}$
- *Assume that the weak limit of the associated bipartite graph* $\mathcal{A}$ *is a BGWT having degree distribution* $(\delta_{\beta d}, \delta_d)$ *and parameter* $\frac{1}{1+\beta}$. *Then:*

  2. *Subject to the Stieltjes transform's convergence, the weak limit of the empirical eigenvalue distribution of* $\frac{1}{d}\mathbf{A}\mathbf{A}^\dagger$ *is a distribution with density*

$$\rho(\lambda, \beta, d) = [1-\beta]^+\delta(\lambda) + \frac{\beta d}{2\pi}\frac{\sqrt{[\lambda-\lambda^-]^+[\lambda^+-\lambda]^+}}{\lambda(\beta d-\lambda)}\ , \qquad (9)$$

where $\lambda^\pm = (\sqrt{\alpha} \pm \sqrt{\gamma})^2$, $\delta(\lambda)$ *is a unit point mass at* $\lambda = 0$, *and* $[z]^+ \triangleq \max\{0, z\}$

Spectral Density of $\frac{1}{d}\mathbf{A}\mathbf{A}^\dagger$ *Cont'd*

- Proof Outline:
  - The proof relies on the observation that the eigenvalues of

$$\tilde{\mathbf{A}}_N^2 = \begin{pmatrix} \mathbf{A}\mathbf{A}^\dagger & \mathbf{0} \\ \mathbf{0} & \mathbf{A}^\dagger\mathbf{A} \end{pmatrix} \quad (10)$$

    are simply the eigenvalues of $\mathbf{A}\mathbf{A}^\dagger$ together with those of $\mathbf{A}^\dagger\mathbf{A}$ (which are in fact the same up to $|K-N|$ additional zero eigenvalues)
  - Furthermore, the limiting Stieltjes transform of the empirical eigenvalue distribution of $\tilde{\mathbf{A}}_N^2$ admits the following relation $zm_{\tilde{\mathbf{A}}^2}(z^2) = m_{\tilde{\mathbf{A}}}(z)$
  - This lets us conclude that $m_{\frac{1}{d}\mathbf{A}\mathbf{A}^\dagger}(z) = \sqrt{\frac{d}{z}}X^a(\sqrt{dz})$, where $X^a(z)$ is obtained via Theorem 1
  - The limiting density is finally obtained following some tedious algebra and using the Stieltjes inversion formula

Special Case 1: The Kesten-McKay Law

- Let the matrix $\mathbf{A}$ be defined as in Theorem 2 with $\beta = 1$
- Consequently: $\alpha = \gamma = \frac{d-1}{d}$
- Then, the limiting spectral density reads

$$\rho(\lambda, 1, d) = \begin{cases} \frac{d\sqrt{4(d-1)-d\lambda}}{2\pi(d-\lambda)\sqrt{d\lambda}}, & 0 \leq \lambda \leq \frac{4(d-1)}{d}, \\ 0, & \text{otherwise} \end{cases} \tag{11}$$

- This conforms with the well-known Kesten-McKay law for regular graphs [McKay (1981)]

Special Case 2: The Marčenko-Pastur Law

- Let the matrix $\mathbf{A}$ be defined as in Theorem 2
- Then, as $d \to \infty$, the limiting spectral density converges to

$$\rho(\lambda, \beta, d \to \infty) = \begin{cases} [1-\beta]^{+}\delta(\lambda) + \frac{\sqrt{(\lambda-\lambda^{-})(\lambda^{+}-\lambda)}}{2\pi\lambda}, & \lambda^{-} \leq \lambda \leq \lambda^{+}, \\ 0, & \text{otherwise}, \end{cases} \quad (12)$$

where $\lambda^{\pm} = (1 \pm \sqrt{\beta})^2$

- This density is nothing but the Marčenko-Pastur law (see, e.g., [Tulino & Verdú (2004)])
- Similar observations were made in [Dumitriu & Johnson (2014)] for $(0,1)$-matrices, where $d \to \infty$, and $d/N \to 0$ at an appropriate rate

Numerical Results: Spectral Density of $\frac{1}{d}\mathbf{A}\mathbf{A}^\mathsf{T}$

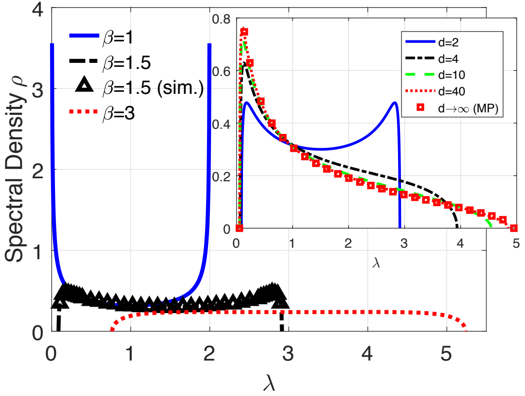

- $d = 2$, simulation results based on matrices obtained via Gallager's (1963) construction of LDPC codes, with $N = 2600$ and $K = 3900$
- Inset: Limiting spectral density for $\beta = 1.5$

Empirical Distribution vs. Limiting Distribution

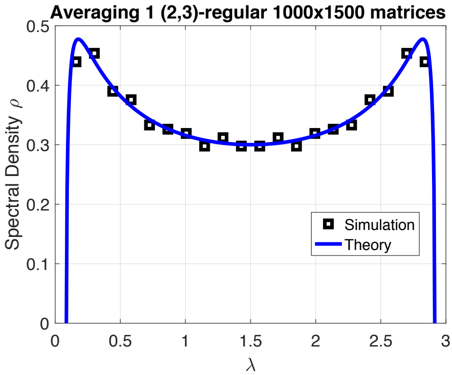

- $d = 2$, $\beta = 1.5$, simulation results based on matrices obtained via Gallager's construction of LDPC codes ($A_{ij} \in \{0, \pm 1\}$)

Empirical Distribution vs. Limiting Distribution *Cont'd*

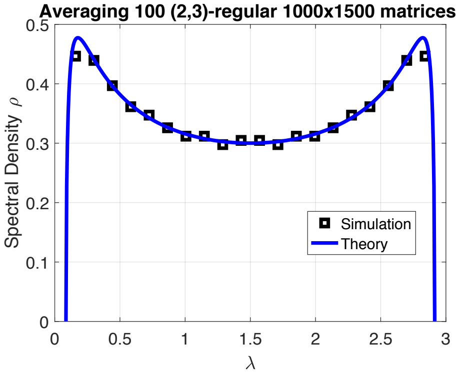

- $d = 2$, $\beta = 1.5$, simulation results based on matrices obtained via Gallager's construction of LDPC codes ($A_{ij} \in \{0, \pm 1\}$)

Empirical Distribution vs. Limiting Distribution *Cont'd*

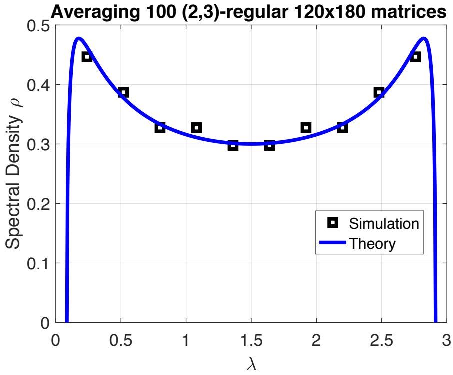

- $d = 2$, $\beta = 1.5$, simulation results based on matrices obtained via Gallager's construction of LDPC codes ($A_{ij} \in \{0, \pm 1\}$)

Optimum Receiver

Optimum Spectral Efficiency

- The fundamental figure of merit for system performance is taken here as the normalized spectral efficiency in bits/sec/Hz per dimension
- For optimum processing this quantity corresponds to the ergodic sum-capacity, given by [Verdú & Shamai (1999)]:

$$C_N^{\text{opt}}(\mathsf{snr}, \beta, d) \triangleq \frac{1}{N} I(\mathbf{x}; \mathbf{y} | \mathbf{A}) = \frac{1}{N} \mathbb{E}\left\{ \log_2 \det \left(\mathbf{I}_N + \frac{\mathsf{snr}}{d} \mathbf{A}\mathbf{A}^\dagger \right) \right\} \quad (13)$$

- Our aim is to characterize $C_N^{\text{opt}}(\mathsf{snr}, \beta, d)$ in the large system limit:

$$N, K \to \infty\ ,\ \frac{K}{N} = \beta \quad (\text{s.t. } \beta d \in \mathbb{N}^+)$$

- We henceforth denote the asymptotic spectral efficiency as

$$C^{\text{opt}}(\mathsf{snr}, \beta, d) \triangleq \lim_{N \to \infty} C_N^{\text{opt}}(\mathsf{snr}, \beta, d) \quad (14)$$

Spectral Efficiency in Closed Form

- Remarkably, Theorem 2 paves the way for a closed form characterization of the asymptotic optimum spectral efficiency

- Let $\mathcal{F}(x,z)$ be defined as [Verdú & Shamai (1999)]

$$\mathcal{F}(x,z) \triangleq \left(\sqrt{x\left(1+\sqrt{z}\right)^2+1}-\sqrt{x\left(1-\sqrt{z}\right)^2+1}\right)^2 \qquad (15)$$

- Let $\mathcal{G}(x,y,z)$ be defined for $x,y,z \in \mathbb{R}^+,\ y \geq (1+\sqrt{z})^2$ as

$$\mathcal{G}(x,y,z) \triangleq \left(\frac{\sqrt{\left(y-(1-\sqrt{z})^2\right)\left(x(1+\sqrt{z})^2+1\right)}-\sqrt{\left(y-(1+\sqrt{z})^2\right)\left(x(1-\sqrt{z})^2+1\right)}}{\sqrt{y-(1-\sqrt{z})^2}-\sqrt{y-(1+\sqrt{z})^2}}\right)^2 \qquad (16)$$

Spectral Efficiency in Closed Form *Cont'd*

Theorem 3

- *Let d, β, α and γ be as in Theorem 2. Further let $\tilde{\beta} \triangleq \frac{\alpha}{\gamma}$ and $\zeta \triangleq \frac{\beta d}{\gamma}$*
- *Then, the optimum spectral efficiency converges as $N \to \infty$ to*

$$\begin{aligned} C^{\text{opt}}(\mathsf{snr}, \beta, d) = & \tfrac{\beta(d-1)+1}{2} \log_2\big(1 + (\gamma + \alpha)\mathsf{snr} - \tfrac{1}{4}\mathcal{F}(\gamma\mathsf{snr}, \tilde{\beta})\big) \\ & + (\beta - 1) \log_2\big(1 + \alpha\mathsf{snr} - \tfrac{1}{4}\mathcal{F}(\gamma\mathsf{snr}, \tilde{\beta})\big) \\ & - \tfrac{\beta(d-1)-1}{2} \log_2 \left(\tfrac{(1+\beta d\, \mathsf{snr})^2}{\mathcal{G}(\gamma\mathsf{snr},\zeta,\tilde{\beta})}\right) \end{aligned} \tag{17}$$

- Although the theorem applies to $2 \le d, \beta d \in \mathbb{N}^+ < \infty$, the convex closure of the respective rates is achievable via time-sharing

Spectral Efficiency in Closed Form *Cont'd*

- Proof Outline:
  - The proof relies on the Skorokhod representation theorem by which we can assume almost sure convergence of the Stieltjes transforms in Theorem 2
  - Note that by Hadamard's inequality

$$\frac{1}{N}\log_2 \det\left(\mathbf{I}_N + \frac{\mathsf{snr}}{d}\mathbf{A}\mathbf{A}^\dagger\right) \leq \log_2(1+\beta\mathsf{snr}) < \infty \tag{18}$$

  - This implies, by uniform integrability and the weak convergence stated in Theorem 2, that the sequence $\frac{1}{N}\log_2 \det\left(\mathbf{I}_N + \frac{\mathsf{snr}}{d}\mathbf{A}\mathbf{A}^\dagger\right)$ converges to

$$\int_0^\infty \log_2(1+\mathsf{snr}\lambda)\rho(\lambda,\beta,d)\,\mathrm{d}\lambda$$

  - Finally, by the bounded convergence theorem we conclude that $C^{\mathrm{opt}}(\mathsf{snr},\beta,d)$ converges to the same limit as well
  - This rigorously establishes the "cavity" method based result of [Shental, Zaidel & Shamai (2017)]. Explicit calculation of the integral finally yields (17)

RS-CDMA: A Reference Result

- Consider the case where $d = N$, and the entries of $\mathbf{A}$ are i.i.d. zero-mean random variables with unit variance (and fourth moment of order $\mathcal{O}(1)$)

- Then, it was shown in [Verdú & Shamai (1999)] that as $N, K \to \infty$, $\frac{K}{N} = \beta$, the optimum spectral efficiency converges to

$$C_{\mathrm{RS}}^{\mathrm{opt}}(\mathsf{snr}, \beta) = \beta \log_2 \left(1 + \mathsf{snr} - \frac{1}{4}\mathcal{F}(\mathsf{snr}, \beta)\right) + \log_2 \left(1 + \beta\mathsf{snr} - \frac{1}{4}\mathcal{F}(\mathsf{snr}, \beta)\right) - \frac{\log_2 \mathrm{e}}{4\,\mathsf{snr}}\mathcal{F}(\mathsf{snr}, \beta) \tag{19}$$

- This result relies on the well known Marčenko-Pastur distribution (e.g., [Tulino & Verdú (2004)]), and does not apply to the sparse setting

Extreme-SNR Characterization

- To complete the asymptotic analysis of the optimum receiver, we also characterize the spectral efficiency in extreme-SNR regimes

- Recall that a spectral efficiency R is approximated in the low-SNR regime as

$$R\left(\frac{E_b}{N_0}\right) \approx \frac{\mathcal{S}_0}{3\,\mathrm{dB}} \left(\frac{E_b}{N_0}\bigg|_{\mathrm{dB}} - \frac{E_b}{N_0}_{\mathrm{min}}\bigg|_{\mathrm{dB}} \right) \tag{20}$$

- Here $\mathcal{S}_0$ denotes the low-SNR slope, $\frac{E_b}{N_0}_{\mathrm{min}}$ is the minimum $\frac{E_b}{N_0}$ that enables reliable communications, and $3\mathrm{dB} \triangleq 10\log_{10}2$ [Shamai & Verdú (2001)]

Extreme-SNR Characterization *Cont'd*

- In the high-SNR regime the spectral efficiency (taken as a function of snr) is approximated as

$$R(\mathsf{snr}) \approx \mathcal{S}_\infty \left(\log_2 \mathsf{snr} - \mathcal{L}_\infty\right) \tag{21}$$

- Here $\mathcal{S}_\infty$ denotes the high-SNR slope (multiplexing gain), and $\mathcal{L}_\infty$ denotes the high-SNR power offset [Shamai & Verdú (2001)]

- Recall that snr and $\frac{E_b}{N_0}$ are related via

$$\beta \mathsf{snr} = R \frac{E_b}{N_0} \tag{22}$$

Extreme-SNR Characterization *Cont'd*

Proposition 1

- *Let d and β be as in Theorem 2. Then, the low-SNR parameters of the optimum receiver read:*

$$\left(\frac{E_b}{N_0}\right)^{\mathrm{opt}}_{\min} = \ln 2 \quad , \quad \mathcal{S}_0^{\mathrm{opt}} = \frac{2\beta d}{d(\beta+1)-1} \tag{23}$$

- *The high-SNR slope of the optimum receiver is given by* $\mathcal{S}_\infty^{\mathrm{opt}} = \min\{1, \beta\}$, *while the high-SNR power offset satisfies*

$$\mathcal{L}_\infty^{\mathrm{opt}} = \begin{cases} \left(\frac{1}{\beta} - 1\right)\log_2(1-\beta) - (d-1)\log_2\left(1 - \frac{1}{d}\right), & \beta < 1 \\ -(d-1)\log_2\left(1 - \frac{1}{d}\right), & \beta = 1 \\ (\beta - 1)\log_2(\beta - 1) - \beta\log_2\beta - (\beta d - 1)\log_2\left(1 - \frac{1}{\beta d}\right), & \beta > 1. \end{cases} \tag{24}$$

RS-CDMA: Extreme-SNR Characterization

- Low-SNR Parameters [Shamai & Verdú (2001)]:

$$\left(\frac{E_b}{N_0}\right)^{\rm opt}_{\rm min,RS} = \ln 2 \quad , \quad \mathcal{S}^{\rm opt}_{0,\rm RS} = \frac{2\beta}{\beta+1} \tag{25}$$

- High-SNR Parameters [Shamai & Verdú (2001)]:

$$\mathcal{S}^{\rm opt}_{\infty,\rm RS} = \min\{1, \beta\} \tag{26}$$

$$\mathcal{L}^{\rm opt}_{\infty,\rm RS} = \begin{cases} \left(\frac{1}{\beta} - 1\right)\log_2(1-\beta) + \log_2 {\rm e}\ , & \beta < 1 \\ \log_2 {\rm e}\ , & \beta = 1 \\ (\beta - 1)\log_2(\beta - 1) - \beta\log_2\beta + \log_2 {\rm e}\ , & \beta > 1 \end{cases} \tag{27}$$

Linear MMSE Receiver

Spectral Efficiency of the LMMSE Receiver

- We now turn to consider the linear minimum mean-square error (LMMSE) receiver
- Namely, an LMMSE front-end is applied to estimate the transmitted signal $\mathbf{x}$, which is then followed by single-user decoders
- The estimation error reflects the equivalent noise
- Useful insights can be obtained by comparing the respective spectral efficiency to that of the optimum receiver
- The comparison can shed light on the potential performance enhancement of near-optimum MPAs, particularly in the overloaded regime

Spectral Efficiency of the LMMSE Receiver

Cont'd

- The error covariance matrix of the LMMSE receiver is given by [Verdú & Shamai (1999)]:

$$\mathbf{M} = (\mathbf{I}_K + \mathsf{snr}\,\mathbf{R})^{-1} \tag{28}$$

where $\mathbf{R} \triangleq \frac{1}{d}\mathbf{A}^\dagger\mathbf{A}$ is the signature crosscorrelation matrix

- Let M_{kk} denote the (k,k)'th element of $\mathbf{R}$, then the signal-to-interference-plus-noise ratio (SINR) at the output of the receiver for user k is

$$\frac{1}{M_{kk}} - 1$$

- The spectral efficiency of the LMMSE receiver thus reads

$$C_K^{\mathrm{mmse}}(\mathsf{snr}, \beta, d) = \beta\,\mathbb{E}\left\{\frac{1}{K}\sum_{k=1}^{K}\log_2\left(\frac{1}{M_{kk}}\right)\right\} \tag{29}$$

Spectral Efficiency of the LMMSE Receiver

Cont'd

Theorem 4

- *Let the definitions and assumptions of Theorem 3 hold*
- *Then, the spectral efficiency of the LMMSE receiver converges as $N \to \infty$ to*

$$C^{\mathrm{mmse}}(\mathsf{snr}, \beta, d) = \beta \log_2 \left(\frac{1+\beta d\, \mathsf{snr}}{1+d\gamma\, \mathsf{snr} - \frac{d\mathcal{F}(\gamma \mathsf{snr}, \tilde{\beta})}{4}} \right) \quad (30)$$

- The time-sharing argument stated for the optimum receiver applies for the LMMSE receiver as well

Spectral Efficiency of the LMMSE Receiver

Cont'd

- Proof Outline:
  - The proof relies on the relation between the resolvent of $\mathbf{R}$, namely $\mathsf{R}_{\mathbf{R}}(z) \triangleq (\mathbf{R} - z\mathbf{I}_K)^{-1}$, $z \in \mathbb{C}^+$, and the error covariance matrix $\mathbf{M}$
  - Following the steps of the proof of Theorem 1 in [Bordenave & Lelarge (2010)], while applying analytic continuation, it can be shown that

$$M_{kk} \xrightarrow{d} \frac{1}{\mathsf{snr}} m_{\mathbf{R}}(-\frac{1}{\mathsf{snr}}) \triangleq M_1 \tag{31}$$

  - Since the random variables $\{M_{kk}\}$ have a bounded strictly positive support, we may eventually conclude that

$$C^{\mathrm{mmse}}(\mathsf{snr}, \beta, d) = \beta \log_2 \left(\frac{1}{M_1}\right) \tag{32}$$

  - The final result follows by direct calculation of M_1

LMMSE Receiver: Extreme-SNR Chacterization

Proposition 2

- *Let d and β be as in Theorem 2*
- *The low-SNR parameters of the LMMSE receiver read:*

$$\left(\frac{E_b}{N_0}\right)_{\min}^{\text{mmse}} = \ln 2 \quad , \quad \mathcal{S}_0^{\text{mmse}} = \frac{2\beta d}{(2\beta+1)d-2} \; . \tag{33}$$

LMMSE Receiver: Extreme-SNR Chacterization *Cont'd*

Proposition 2 (*Cont'd*)

- *The high-SNR slope of the LMMSE receiver is given by*

$$\mathcal{S}_{\infty}^{\text{mmse}} = \begin{cases} \beta, & \beta < 1 \\ \frac{1}{2}, & \beta = 1 \\ 0, & \beta > 1 \end{cases} \tag{34}$$

while the high-SNR power offset satisfies

$$\mathcal{L}_{\infty}^{\text{mmse}} = \begin{cases} \log_2\left(\frac{1}{1-\beta}\right) + \log_2\left(\frac{d-1}{d}\right), & \beta < 1 \\ \log_2\left(\frac{d-1}{d}\right), & \beta = 1. \end{cases} \tag{35}$$

RS-CDMA: The LMMSE Receiver

- The spectral efficiency of the LMMSE receiver in the RS-CDMA setting is given by [Verdú & Shamai (1999)]:

$$C_{\mathrm{RS}}^{\mathrm{mmse}}(\mathsf{snr},\beta) = \beta \log_2 \left(1 + \mathsf{snr} - \frac{1}{4}\mathcal{F}(\mathsf{snr},\beta)\right) \tag{36}$$

- Low-SNR Parameters:

$$\left(\frac{E_b}{N_0}\right)_{\min,\mathrm{RS}}^{\mathrm{mmse}} = \ln 2 \quad , \quad \mathcal{S}_{0,\mathrm{RS}}^{\mathrm{mmse}} = \frac{2\beta}{2\beta+1} \tag{37}$$

- High-SNR Parameters:

$$\mathcal{S}_{\infty,\mathrm{RS}}^{\mathrm{mmse}} = \begin{cases} \beta \, , & \beta < 1 \\ \frac{1}{2} \, , & \beta = 1 \\ 0 \, , & \beta > 1 \end{cases} \quad , \quad \mathcal{L}_{\infty,\mathrm{RS}}^{\mathrm{mmse}} = \begin{cases} \log \frac{1}{1-\beta} \, , & \beta < 1 \\ 0 \, , & \beta = 1 \end{cases} \tag{38}$$

Numerical Results

Limiting Throughput vs. System Load: The Underloaded Regime ($\frac{E_b}{N_0} = 10\text{dB}$)

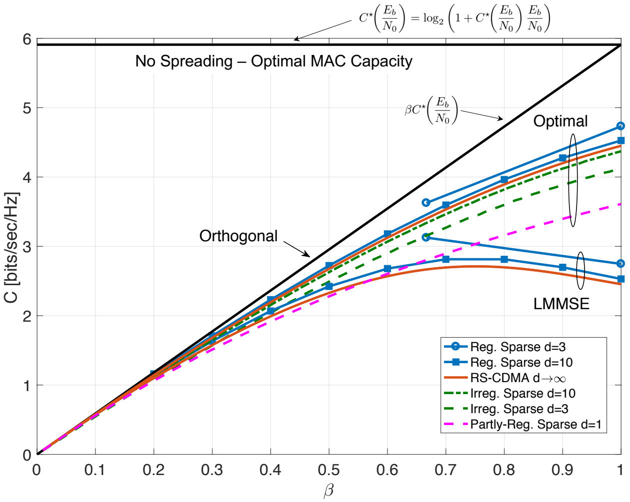

Limiting Throughput vs. System Load: The Overloaded Regime ($\frac{E_b}{N_0} = 10\text{dB}$)

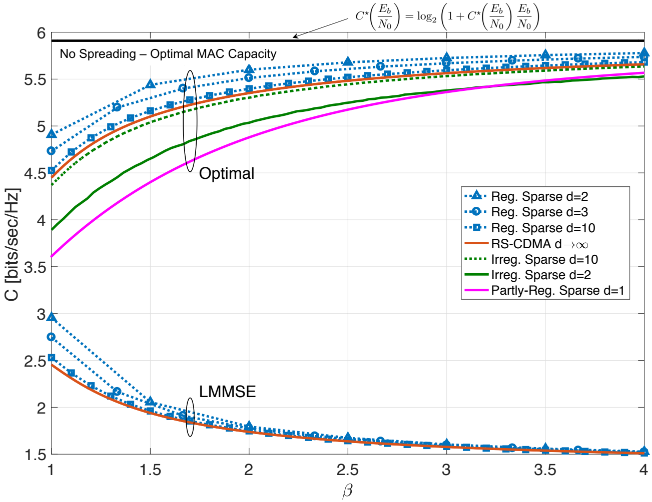

Limiting Throughput vs. $\frac{E_b}{N_0}$ $(\beta = 1.5)$

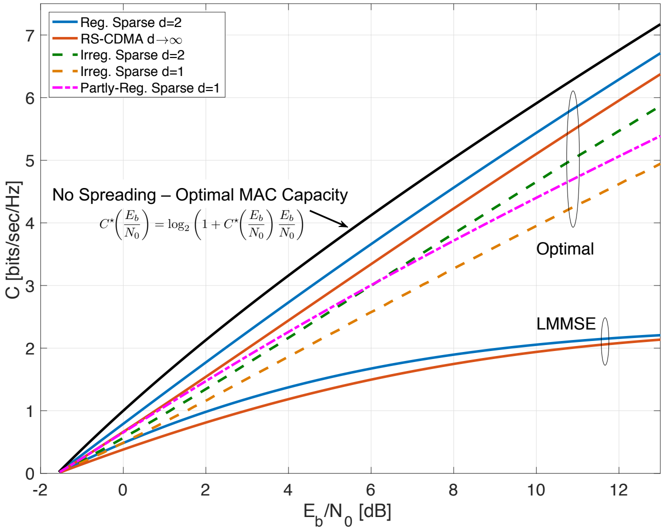

Concluding Remarks

Concluding Remarks

- Understanding the fundamental limitations of the various technologies suggested for future 5G systems is crucial for efficient state-of-the-art designs

- An insightful attempt in this framework was presented by examining the advantages of regular LDCD-NOMA

- Considering the large system limit, the achievable total throughput of regular LDCD-NOMA was analytically characterized in closed form while:
  - Assuming random signature matrices with i.i.d. nonzero entries residing on the unit-circle in $\mathbb{C}$
  - Harnessing tools from the spectral theory of large random graphs

Concluding Remarks *Cont'd*

- The underlying model is markedly different from previously analyzed settings:
  - The random matrices are sparse, as opposed to standard dense RS-CDMA (governed by the Marčenko-Pastur distribution [Verdú & Shamai (1999)])
  - The matrix entries are not i.i.d. as opposed to Poissonian irregular sparse spreading (see, e.g., [Yoshida & Tanaka (2006)])
  - The number of nonzero entries in each column (row) is identical and remains fixed (deterministic) in the large system limit
  - This comes in contrast to the sparse settings considered, e.g., in:
    - [Guo, Baron & Shamai (2009)]: Limiting average sparsity amounts to a fixed (small) fraction of the dimensions (linear scaling)
    - [Guo & Wang (2008)]: Number of nonzero column entries amounts to a vanishing fraction of the dimension, but is still infinite in the large system limit

Concluding Remarks *Cont'd*

- Regular sparse NOMA potentially leads to significant performance enhancement over both irregular spreading and RS-CDMA (dense NOMA)
- This is of particular importance in view of the fact that optimum performance can be approached using practical MPAs even in overloaded regimes
- Our observations thus advocate employing regular schemes (e.g., SCMA[2]) as a key practical tool for enhancing performance of future overloaded systems
- Regular schemes require, however, some kind of coordination or central scheduling and may therefore pose some additional practical challenges

[2] Sparse Code Multiple Access

Outlook

- Several extensions of the results are currently investigated, accounting for:
  - Fading channel models
  - Impact of multiple transmit-receive antennas (MIMO-NOMA), and in particular massive-MIMO (e.g., [Liu et al. (2018)])
  - Multi-cell NOMA, where implications of inter-cell interference and joint multi-cell processing should be accounted for (see, e.g., [Shin et al. (2017)])
- Additional challenging aspects of NOMA include, e.g.:
  - Coordination and scheduling for maintaining regularity
  - Practical impairments such as imperfect CSI
  - I-MMSE relations [Guo, Shamai & Verdú (2013)]
  - Physical layer security (e.g., see [Gomez et al. (2017)], [Zhang et al. (2018)])
  - Combining power-domain and code-domain NOMA (e.g., [Qin et al. (2018-1)])

Outlook *Cont'd*

- Sparse channel models are obviously not restricted to NOMA and have a variety of applications
- Considering, e.g., the compressed sensing framework (see [Qin et al. (2018-2)] for a recent survey), such models can be applied to:
  - Spectrum sensing in cognitive radio networks
  - Data collection in wireless sensor networks
  - Channel estimation and feedback in massive MIMO

OUTLOOK *Cont'd*

- In particular, sparse-graph codes were recently investigated in the context of speeding up learning and recovery of sparse signals [Ramchadran, ISIT'2018]:
  - Low-complexity Discrete Fourier Transform (DFT) computation for sparse spectrum signals (e.g., [Pawar & Ramchadran (2013, 2014, 2018)])
  - Neighbor discovery for Internet-of-Things (IoT) [Lee, Pedarsani & Ramchadran (2016)], [Chandrasekher et al. (2017)]
  - Minimum-rate spectrum-blind sampling [Öçal, Li and Ramchadran (2016)]
- Sparse representations in the time-frequency (delay-Doppler) domain are also of great interest, e.g.:
  - Representing underspread WSS uncorrelated scattering channels [Durisi et al. (2011)]
  - Orthogonal time frequency space (OTFS) modulation [Monk et al. (2016)]

Thank You!

References

References I

[1] L. Dai, B. Wang, Y. Yuan, S. Han, C.-L. I, and Z. Wang, "Non-orthogonal multiple access for 5G: Solutions, challenges, opportunities, and future research trends," *IEEE Commun. Mag.*, vol. 53, no. 9, pp. 74–81, Sep. 2015.

[2] R. Hoshyar, R. Razavi, and M. Al-Imari, "LDS-OFDM an efficient multiple access technique," in *Proc. 2010 IEEE 71st Veh. Technol. Conf.*, May 2010, pp. 1–5.

[3] A. Bayesteh, H. Nikopour, M. Taherzadeh, H. Baligh, and J. Ma, "Low complexity techniques for SCMA detection," in *2015 IEEE Globecom Workshops (GC Wkshps)*, Dec. 2015, pp. 1–6.

[4] M. Taherzadeh, H. Nikopour, A. Bayesteh, and H. Baligh, "SCMA codebook design," in *Proc. 2014 IEEE 80th Veh. Technol. Conf. (VTC2014-Fall)*, Sep. 2014, pp. 1–5.

[5] Z. Ding, M. Peng, and H. V. Poor, "Cooperative non-orthogonal multiple access in 5G systems," *IEEE Comm. Letters*, vol. 19, no. 8, pp. 1462–1465, Aug. 2015.

[6] S. M. R. Islam, J. M. Kim, and K. S. Kwak, "On non-orthogonal multiple access (NOMA) in 5G systems," *The Journal of Korean Institute of Communications and Information Sciences*, vol. 40, no. 12, pp. 2549–2558, 2015.

References II

[7] R. C. Kizilirmak, "On-orthogonal multiple access (NOMA) for 5G networks," in *Towards 5G Wireless Networks - A Physical Layer Perspective*, H. K. Bizaki, Ed. InTech, 2016.

[8] N. Bhuvanasundaram, H. X. Nguyen, R. Trestian, and Q.-T. Vien, "Non-orthogonal multiple access schemes for next-generation 5G networks: A survey," in *5G Radio Access Networks: Centralized RAN, Cloud-RAN and Virtualization of Small Cells*, H. Venkataraman and R. Trestian, Eds. CRC Press, 2017.

[9] M. Zeng, A. Yadav, O. A. Dobre, G. I. Tsiropoulos, and H. V. Poor, "Capacity comparison between MIMO-NOMA and MIMO-OMA with multiple users in a cluster," *IEEE J. Sel. Topics Commun.*, 2017, Accepted for publication.

[10] Y. Xu, C. Shen, Z. Ding, X. Sun, S. Yan, G. Zhu, and Z. Zhong, "Joint beamforming and power splitting control in downlink cooperative SWIPT NOMA systems," *IEEE Trans. Signal Process.*, 2017, To Appear.

References III

[11] P. Xu, Z. Ding, and H. V. Poor, "Information theoretic perspectives on non-orthogonal multiple access (NOMA)," in *Information-Theoretic Perspectives on 5G Systems and Beyond*, I. Marić, O. Simeone, and S. Shamai (Shitz), Eds. Cambridge University Press, 2018.

[12] M. Yoshida and T. Tanaka, "Analysis of sparsely-spread CDMA via statistical mechanics," in *Proc. 2006 IEEE Int. Symp. Inf. Theory (ISIT'06)*, Seatle, WA, Jul. 2006, pp. 2378–2382.

[13] S. Verdú and S. Shamai (Shitz), "Spectral efficiency of CDMA with random spreading," *IEEE Trans. Inf. Theory*, vol. 45, no. 2, pp. 622–640, Mar. 1999.

[14] J. Raymond and D. Saad, "Sparsely spread CDMA - a statistical mechanics-based analysis," *J. Phys. A: Mathematical and theoretical*, vol. 40, no. 41, p. 12315, 2007.

[15] G. C. Ferrante and M.-G. Di Benedetto, "Spectral efficiency of random time-hopping CDMA," *IEEE Trans. Inf. Theory*, vol. 61, no. 12, pp. 6643–6662, Dec. 2015.

[16] C. D. Godsil and B. Mohar, "Walk generating functions and spectral measures of infinite graphs," *Linear Algebra Appl.*, vol. 107, pp. 191–206, 1988.

References IV

[17] T. Rogers, I. P. Castillo, R. Kühn, and K. Takeda, "Cavity approach to the spectral density of sparse symmetric random matrices," *Phys. Rev. E*, vol. 78, p. 031116, Sep. 2008.

[18] T. Rogers, "New results on the spectral density of random matrices," PhD Thesis, King's College, London, UK, Jul. 2010.

[19] C. Bordenave and M. Lelarge, "Resolvent of large random graphs," *Random Structures & Algorithms*, vol. 37, no. 3, pp. 332–352, 2010.

[20] T. Richardson and R. Urbanke, *Modern Coding Theory*. Cambridge University Press, 2008.

[21] R. R. Far, T. Oraby, W. Bryc, and R. Speicher, "On slow-fading MIMO systems with nonseparable correlation," *IEEE Trans. Inf. Theory*, vol. 54, no. 2, pp. 544–553, Feb. 2008.

[22] H. Mizuno and I. Sato, "The semicircle law for semiregular bipartite graphs," *J. Comb. Theory, Ser. A*, vol. 101, no. 2, pp. 174–190, 2003.

[23] M. Mézard, G. Parisi, and M. Virasoro, "SK model: The replica solution without replicas," *Europhys. Lett*, vol. 1, no. 2, pp. 77–82, 1986.

References V

[24] B. D. McKay, "The expected eigenvalue distribution of a large regular graph," *Linear Algebra Appl.*, vol. 40, pp. 203 – 216, 1981.

[25] A. M. Tulino and S. Verdú, "Random matrix theory and wireless communications," *Found. Trends Commun. Inf. Theory*, vol. 1, no. 1, pp. 1–182, 2004.

[26] R. Couillet and M. Debbah, *Random Matrix Methods for Wireless Communications*. Cambridge University Press, 2011.

[27] I. Dumitriu and T. Johnson, "The Marčenko-Pastur law for sparse random bipartite biregular graphs," *Random Structures & Algorithms*, 2014.

[28] O. Shental, B. M. Zaidel, and S. Shamai (Shitz), "Low-density code-domain NOMA: Better be regular," in *Proc. 2017 IEEE Int. Symp. Inf. Theory (ISIT'17)*, Aachen, Germany, Jun. 25–30, 2017.

[29] A. Dembo, A. Montanari, and N. Sun, "Factor models on locally tree-like graphs," *Ann. Probab.*, vol. 41, no. 6, pp. 4162–4213, 2013.

References VI

[30] D. Guo, S. Shamai (Shitz), and S. Verdú, "The interplay between information and estimation measures," *Found. and Trends in Signal Process., Now Publishers Inc., Hanover MA*, vol. 6, no. 4, pp. 243–429, 2012.

[31] G. Gómez, F. J. Martin-Vega, F. J. López-Martínez, Y. Liu, and M. Elkashlan, "Uplink NOMA in large-scale systems: Coverage and physical layer security," *CoRR*, vol. abs/1709.04693, 2017. [Online]. Available: http://arxiv.org/abs/1709.04693

[32] H. Zhang, N. Yang, K. Long, M. Pan, G. K. Karagiannidis, and V. C. M. Leung, "Secure communications in NOMA system: Subcarrier assignment and power allocation," *ArXiv e-prints*, Jan. 2018. [Online]. Available: https://arxiv.org/abs/1801.04441v1

[33] Y. Liu, H. Xing, C. Pan, A. Nallanathan, M. Elkashlan, and L. Hanzo, "Multiple antenna assisted non-orthogonal multiple access," *IEEE Wireless Commun.*, 2018, Accepted for publication.

[34] W. Shin, M. Vaezi, B. Lee, D. J. Love, J. Lee, and H. V. Poor, "Non-orthogonal multiple access in multi-cell networks: Theory, performance, and practical challenges," *IEEE Comm. Mag.*, pp. 176–183, Oct. 2017.

References VII

[35] Z. Qin, X. Yue, Y. Liu, Z. Ding, and A. Nallanathan, "User association and resource allocation in unified non-orthogonal multiple access enabled heterogeneous ultra dense networks," *ArXiv e-prints*, Jan. 2018. [Online]. Available: https://arxiv.org/abs/1801.08198v1

[36] Z. Qin, J. Fan, Y. Liu, Y. Gao, and G. Y. Li, "Sparse representation for wireless communications," *ArXiv e-prints*, Jan. 2018. [Online]. Available: https://arxiv.org/abs/1801.08206v1

[37] S. Pawar and K. Ramchadran, "Computing a k-sparse n-length Discrete Fourier Transform using at most $4k$ samples and $o(k \log k)$ complexity," in *Proc. 2013 IEEE Int. Symp. Inf. Theory (ISIT'13)*, Istanbul, Turkey, Jul. 7–12, 2013, pp. 464–468.

[38] ——, "A robust R-FFAST framework for computing a k-sparse n-length DFT in $o(k \log n)$ sample complexity using sparse-graph codes," in *Proc. 2014 IEEE Int. Symp. Inf. Theory (ISIT'14)*, Honolulu, HI, USA, Jun. 29 – Jul. 4, 2014, pp. 1852–1856.

[39] ——, "R-FFAST: A robust sub-linear time algorithm for computing a sparse DFT," *IEEE Trans. Inf. Theory*, vol. 64, no. 1, pp. 451–466, Jan. 2018.

References VIII

[40] K. Lee, R. Pedarsani, and K. Ramchadran, "SAFFRON: A fast, efficient, and robust framework for group testing based on sparse-graph codes," in *Proc. 2016 IEEE Int. Symp. Inf. Theory (ISIT'16)*, Barcelona, Spain, Jul. 10–15, 2016, pp. 2873–2877.

[41] K. Chandrasekher, K. Lee, P. Kairouz, R. Pedarsani, and K. Ramchadran, "Asynchronous and noncoherent neighbor discovery for the IoT using sparse-graph codes," in *Proc. Int. Conf. Commun.*, Paris, France, May 21–25, 2017.

[42] O. Öçal, X. Li, and K. Ramchadran, "A sparse-graph-coded filter bank approach to minimum-rate spectrum-blind sampling," in *Proc. 2016 IEEE Int. Conf. on Acoust., Speech and Signal Process. (ICASSP)*, Shanghai, China, Mar. 20–25 2016, pp. 6365–6369.

[43] G. Durisi, V. I. Morgenshtern, H. Bölcskei, U. G. Schuster, and S. Shamai (Shitz), "Information theory of underspread WSSUS channels," in *Wireless Communications over Rapidly Time-Varying Channels*, F. Hlawatsch and G. Matz, Eds. Academic Press, 2011, ch. 2.

[44] A. Monk, R. Hadani, M. Tsatsanis, and S. Rakib, "OTFS - orthogonal time frequency space," *CoRR*, Aug. 2016. [Online]. Available: `https://arxiv.org/abs/1608.02993`